LAND DEGRADATION & DEVELOPMENT
Land Degrad. Develop. **28**: 309–316 (2017)
Published online in Wiley Online Library (wileyonlinelibrary.com) **DOI**: 10.1002/ldr.2635

LEGUME GRASSLANDS PROMOTE PRECIPITATION INFILTRATION BETTER THAN GRAMINEOUS GRASSLANDS IN ARID REGIONS

Ze Huang[1,2], Fu-Ping Tian[4], Gao-Lin Wu[1,3]*, Yu Liu[1,3], Zhi-Qiang Dang[1,3]

[1]*State Key Laboratory of Soil Erosion and Dryland Farming on the Loess Plateau, Northwest A&F University, Yangling, Shaanxi 712100, PR China*
[2]*College of Forestry, Northwest A&F University, Yangling, Shaanxi 712100, PR China*
[3]*Institute of Soil and Water Conservation, Chinese Academy of Sciences and Ministry of Water Resource, Yangling, Shaanxi 712100, PR China*
[4]*Lanzhou Institute of Husbandry and Pharmaceutical Sciences of Chinese Academy of Agricultural Sciences, The Lanzhou Scientific Observation and Experiment Field Station of Ministry of Agriculture for Ecological System in the Loess Plateau Area, Lanzhou, Gansu 730050, PR China*

Received 19 June 2016; Revised 18 September 2016; Accepted 19 September 2016

ABSTRACT

Precipitation infiltration is the most important process for soil water supply of vegetation in the arid regions. Higher infiltration rate is advantageous for vegetation growth and maintenance in the arid areas. Four grassland types (*Medicago sativa*, *Agropyron cristatum*, *Caragana korshinskii* and *Stipa capillata*) were selected in this study. Results showed that the infiltration capacity in the legume grasslands was about 30% higher than in the gramineous grasslands and the difference was significant ($p < 0{\cdot}05$). Furthermore, the infiltration rate in legume shrub-grassland was 16% less than the legume grasslands, but the difference was not significant ($p > 0{\cdot}05$). The below-ground biomass, total porosity, capillary porosity, soil organic matters and soil aggregate were the main factors to determine the soil infiltration rates. The capillary porosity and soil aggregate of the top soil presented significant negative effects on soil infiltration rate ($p < 0{\cdot}05$). The below-ground biomass in 10–30 cm soil layer was the most important factor, which significantly and positively correlates with the soil infiltration rate ($p < 0{\cdot}01$). It is possible to conclude that the legume grasslands presented the higher soil infiltration rate and promoted precipitation infiltration in the studied area. And the legume grasslands might be a more suitable option for vegetation restoration from the perspective of soil infiltration and water supply in the arid regions.

KEY WORDS: arid area; soil infiltration; soil characteristics; below-ground biomass; soil organic matters

INTRODUCTION

Precipitation infiltration is the most important process for soil water supply in the arid regions (Leung *et al*., 2015). The efficiency of the rainfall transform into soil water highly depends on the infiltration capacity, and this process is very important for soil water replenishment in water shortage regions (Wang *et al*., 2007; Siltecho *et al*., 2015; Wang *et al*., 2016). Thus, the research of soil infiltration capacity is a vital issue for vegetation maintenance and sustainable development.

Many engineering measures have been taken up to increase infiltration and decrease runoff for preventing soil erosion. Vegetation restoration is one of the most important and effective measures to control soil and water loss (Yu *et al*., 2015). The restoration of natural grasslands and the establishment of artificial grasslands are very common in arid areas of the world. Vegetation types play an important role in influencing soil hydraulic properties (Mao & Cherkauer, 2009; Gonzalez-Sosa *et al*., 2010). Several studies have found that runoff and soil erosion are highly related to plant cover levels (McIvor *et al*., 1995; Podwojewski *et al*., 2011). Grassland degradation leads to the reduction of vegetation cover and thus soil erosion increased (Mchunu & Chaplot, 2012). The effects of plant roots on reducing soil erosion are also a crucial factor. Different grasslands cover and roots distribution may result in modification of soil properties and then have a vital effect on infiltration (Angers & Caron, 1998; Vervoort *et al*., 2001; Wang *et al*., 2007; Bormann & Klaassen, 2008; Zhao *et al*., 2013; Yu *et al*., 2015). Many studies have found that the main soil properties influencing soil infiltration by grassland types were bulk density (BD) (Neris *et al*., 2012), soil organic matters (SOMs) (Hu *et al*., 2009), initial water content (Wang *et al*., 2007), soil aggregation (Abu-Hamdeh *et al*., 2006), porosity (Kodešová *et al*., 2011), macropores (Wahl *et al*., 2003; Weiler & Naef, 2003) and saturated hydraulic conductivity (Alaoui *et al*., 2011). The steady infiltration rate (SIR) is significantly and logarithmically correlated with SOMs and macroaggregate (Franzluebbers, 2002; Zhao *et al*., 2013). Alaoui (2015) has reported that the interaction between BD and macroporsity may also promote the soil water infiltration. Cerdà (1996) has found that infiltration is 25% lower in wet season than drought season, because of the increase of soil moisture (Cerdà, 1997). On the contrary, some scholars have reported that soil texture is not correlated with infiltration capacity, and soil BD has little or no relationship to water flow through macropores (Meek *et al*., 1989; Fischer *et al*., 2014).

Different grass types, such as legume and Gramineae plants, have different vegetation cover and roots

*Correspondence to: G.-L. Wu, Institute of Soil and Water Conservation, Chinese Academy of Sciences and Ministry of Water Resource, Yangling, Shaanxi 712100, PR China.
E-mail: gaolinwu@gmail.com

Table I. Soil BD, TP, CP, NCP, SA (>0·25 mm) and SOM (mean ± SD) at the depth of 0–30 cm of different grasslands

	Soil depth (cm)	BD (g cm^{-3})	TP (%)	CP (%)	NCP (%)	SA (%)	SOM (g kg^{-1})
Medicago sativa	0–10	1·28 ± 0·02 a	51·62 ± 0·70 c	24·80 ± 0·36 b	26·82 ± 1·06 b	61·46 ± 2·43 b	30·96 ± 3·72 a
	10–20	1·40 ± 0·06 a	47·36 ± 2·21 b	26·99 ± 1·13 ab	20·37 ± 3·35 c	45·19 ± 10·13 b	29·75 ± 9·80 a
	20–30	1·37 ± 0·07 ab	48·26 ± 2·52 bc	26·52 ± 1·29 b	21·74 ± 3·82 a	47·45 ± 2·75 a	16·37 ± 4·33 ab
Agropyron cristatum	0–10	1·20 ± 0·02 bc	54·68 ± 0·72 ab	27·14 ± 0·43 a	27·54 ± 1·15 b	62·65 ± 5·20 b	30·27 ± 4·88 a
	10–20	1·25 ± 0·02 b	52·88 ± 0·92 a	28·22 ± 0·55 a	24·66 ± 1·47 bc	43·09 ± 6·19 b	24·11 ± 3·69 ab
	20–30	1·44 ± 0·11 a	45·53 ± 4·13 c	32·62 ± 2·48 a	12·92 ± 6·61 b	24·72 ± 2·51 b	20·61 ± 4·79 a
Stipa capillata	0–10	1·24 ± 0·02 ab	53·08 ± 0·7 bc	27·70 ± 0·41 a	25·39 ± 1·11 b	80·84 ± 13·40 a	31·77 ± 1·41 a
	10–20	1·19 ± 0·04 b	55·27 ± 1·55 a	26·4 ± 0·92 ab	28·87 ± 2·47 ab	64·08 ± 3·81a	23·24 ± 0·47 ab
	20–30	1·28 ± 0·01 bc	51·70 ± 0·56 ab	28·51 ± 0·33 b	23·18 ± 0·88 a	33·13 ± 11·05b	16·10 ± 0·12 ab
Caragana korshinskii	0–10	1·14 ± 0·07 c	57·03 ± 2·67 a	24·78 ± 1·54 b	32·26 ± 4·21 a	51·55 ± 11·34 b	18·35 ± 0·54 b
	10–20	1·16 ± 0·07 b	56·10 ± 2·76 a	25·31 ± 1·59 b	30·79 ± 4·35 a	48·42 ± 7·41 b	17·41 ± 1·17 b
	20–30	1·21 ± 0·03 c	54·50 ± 1·27 a	26·23 ± 0·73 b	28·27 ± 2·01 a	24·68 ± 8·27 b	13·27 ± 0·41 b

BD, bulk density; TP, total porosity; CP, capillary porosity; NCP, non-capillary porosity; SA, soil aggregate; SOM, soil organic matter.
Values followed by a different letter at the same soil depth in different grassland are significantly different at the 0·05 level (LSD).

distribution at the similar natural environmental conditions. Legumes are available for enhancing grassland production and community diversity (Daniel *et al*., 1999), improving soil structure, decreasing soil BD (Lal, 1996) and increasing soil organic carbon storage with higher above-ground and below-ground biomass (BGB) (Wu *et al*., 2016a). Tab roots decay of leguminous would form stable macropore; it is advantageous for rainfall infiltration (Archer *et al*., 2002). Additionally, grasslands sustainable development is commonly associated with soil water availability in the arid region (Liu *et al*., 2010; Rodriguez-Iturbe, 2000). Higher infiltration rate has accelerated rainfall converting and supplying to the soil water that is conductive to rehabilitate and sustainable development of grasslands in arid regions (Bochet *et al*., 2006). Dabney *et al*. (2001) had summarized predecessor's research results that deep-rooted plants can effectively increase the effective root depth and subsoil water storage capacity. The infiltration rate is correlated with root characteristics, and differences in rooting depth and size would cause differences of water distribution and water infiltration rate (Archer *et al*., 2002; Leung *et al*., 2015). Consequently, according to these issues, it is of great importance to evaluate the infiltration capacity and soil water supply capability under different grassland types in the arid region. And the significant factors determining the infiltration rates at different infiltration stages also need

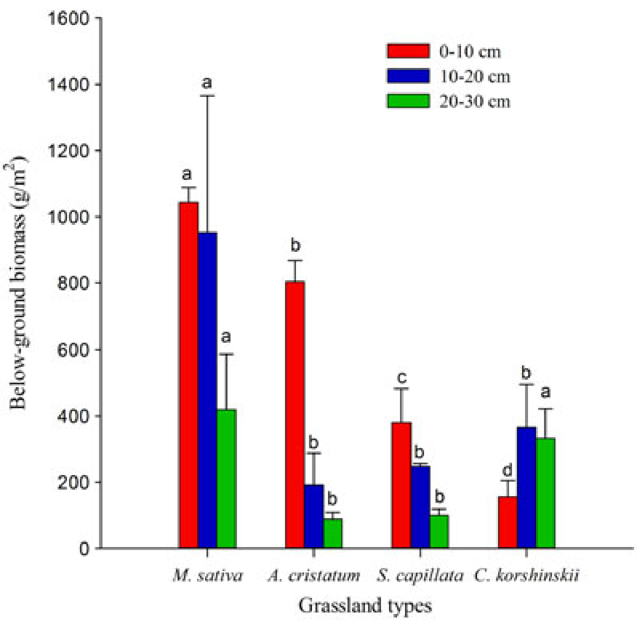

Figure 1. Below-ground biomass at the depth of 0–30 cm (mean ± SD) for different grassland types. Values with a different letter in the same soil depth are significantly different at the 0·05 level. This figure is available in colour online at wileyonlinelibrary.com/journal/ldr

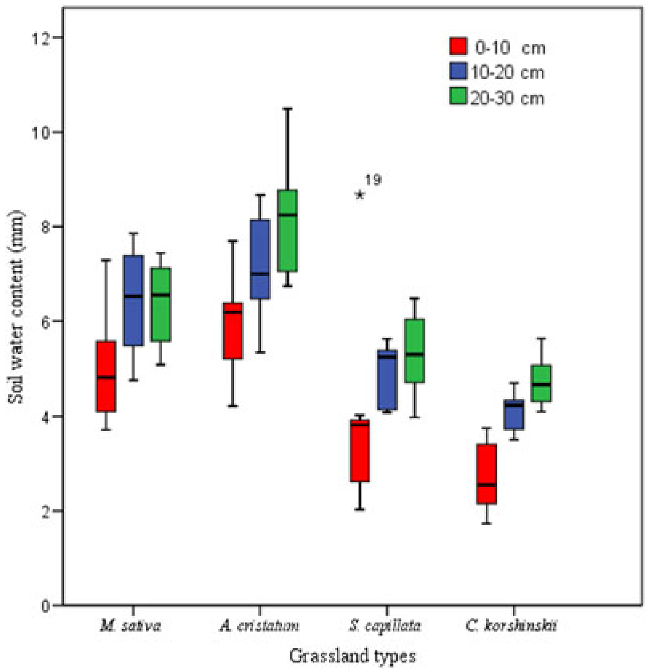

Figure 2. Soil water content at the depth of 0–30 cm (mean ± SD) for different grasslands. This figure is available in colour online at wileyonlinelibrary.com/journal/ldr

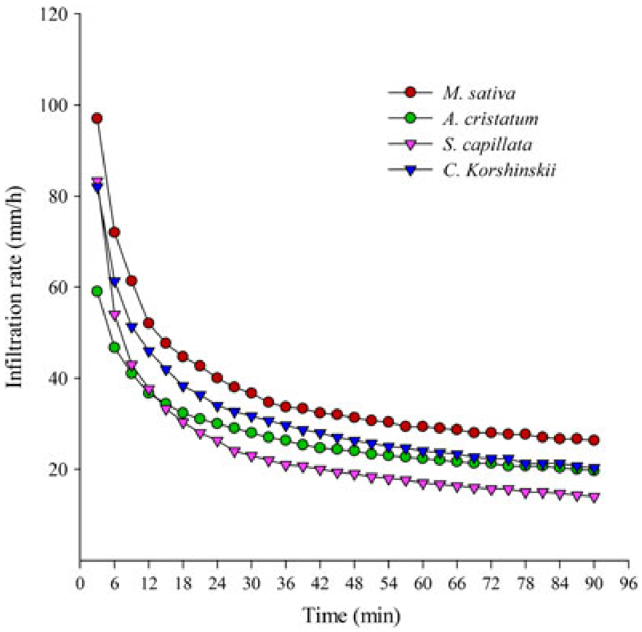

Figure 3. Soil infiltration rates under different grasslands. This figure is available in colour online at wileyonlinelibrary.com/journal/ldr

to be studied. Despite the known effects of soil characteristics on soil infiltration, the knowledge is still lacking to study the relationship between soil infiltration features and soil characteristics under different grassland types in the arid areas.

Therefore, in this point of view, the aims of this study are to determine the effects of grassland types and the main soil characteristics on soil infiltration features in arid area, to find out the significant influence factors on infiltration rate and to determine the suitable vegetation restoration in terms of rainfall infiltration and soil water supply.

MATERIALS AND METHODS

Study Sites

This study was conducted in the Key Field Observation Station of Ecological Environment of the Ministry of Agriculture on the Loess Plateau, which is located in the Gongjiawan of Lanzhou city of Gansu Province in China (36°01′N, 103°45′W). This area belongs to the arid hilly and gully regions on the Loess Plateau. The altitude of the study area ranges from 1698 to 1823 m. Mean annual precipitation is 324·5 mm, most of which falls between July and September. The annual evaporation is approximately 1450·0 mm and the sunshine duration is 2651·4 h. The mean annual air temperature is 9·3 °C, the lowest temperatures being −23·1 °C and the highest temperatures being 39·1 °C. The growing season is from April to September. Mainly, soil type is the loessal soil, and the field moisture capacity is about 19·3–22·6%. The native grassland ecosystem is mainly dominated by *Stipa capillata* in this area.

Experimental Design

Based on field survey of grassland types on the Loess Plateau, we selected three typical artificial grasslands (*Medicago sativa*, *Agropyron cristatum* and the *Caragana korshinskii* shrub-grassland) that were widely planted in this area. The main natural grassland (*S. capillata*) was selected in this study. *M. sativa* grassland is a quality perennial legume grassland, *A. cristatum* grassland is a perennial Gramineae grassland, and *C. korshinskii* grassland is the good shrubs for improving grassland ecosystem, which are widely planted in this area. Each grassland type has three parallels. *M. sativa* and *C. korshinskii* were belonging to the leguminosae and very common artificial vegetation in the arid region of the Loess Plateau. *A. cristatum* and *S. capillata* were the gramineous grasslands that were widely occurred in this area, while *S. capillata* was the typical native grassland.

The test of infiltration process was conducted in June; we randomly selected three parallel (1 m × 1 m) quadrats in each plot, harvested the grasses at the soil level and put into an envelope, then weighed fresh and dried at 75 °C for 48 h as above-ground biomass. We used 9-cm diameter root augur to measure BGB at the depth of 0–100 cm and every 10 cm intervals, and three parallel were sampled for each plot. Three samples were taken at the same layer and then mixed to create a single sample. Using a 2 mm sieve to separate the plant roots from soil. The separated roots were dried at 75 °C for 48 h and then weighed.

Soil Sampling and Analysis

Surface soil samples were collected at the depth of 0–30 cm and every 10 cm intervals. In each plot, three samples were randomly collected, and three soil cores were randomly taken with a stainless cylinder for laboratory assays of soil

Table II. Soil infiltration rates (mean ± SD) of different grasslands

	AIR ($mm\,h^{-1}$)	SIR ($mm\,h^{-1}$)	IR I ($mm\,h^{-1}$)	IR II ($mm\,h^{-1}$)	IR III ($mm\,h^{-1}$)
Medicago sativa	37·49 ± 8·38 a	26·87 ± 6·90 a	66·00 ± 9·50 a	36·80 ± 9·21 a	29·23 ± 7·78 a
Agropyron cristatum	27·31 ± 4·69 b	20·27 ± 4·24 ab	43·53 ± 5·40 c	27·80 ± 4·90 ab	22·23 ± 4·38 ab
Stipa capillata	24·31 ± 1·15 b	14·60 ± 1·11 b	50·27 ± 2·66 bc	23·47 ± 1·32 b	17·03 ± 1·30 b
Caragana korshinskii	31·49 ± 2·86 ab	21·00 ± 2·42 ab	56·53 ± 3·45 ab	31·70 ± 3·10 ab	24·00 ± 2·65 ab

AIR: average infiltration rate (0–90 min); SIR: steady infiltration rate (75–90 min); IR I, IR II and IR III: average infiltration rates during stages I (0–15 min), II (15–45 min) and III (45–75 min).
Values followed by a different letter in the same column were significantly different at the 0·05 level (LSD).

Table III. Matrix showing correlations between soil characteristics and infiltration rates of AIR, SIR, IR I, IR II and IR III

	SOM10	SOM20	SOM30	SA10	SA20	SA30	BD10	TP10	CP10	NCP10	BD20	TP20
AIR	0·09	0·662[a]	0·248	−0·215	−0·034	0·57	−0·027	0·027	−0·780[b]	0·386	0·307	−0·307
SIR	0·142	0·680[a]	0·384	−0·250	−0·160	0·529	−0·020	0·020	−0·717[b]	0·351	0·352	−0·352
IR I	0·049	0·559	−0·054	−0·110	0·153	0·653[a]	0·129	−0·129	−0·752[b]	0·258	0·316	−0·316
IR II	0·067	0·648[a]	0·288	−0·234	−0·050	0·513	−0·101	0·101	−0·777[b]	0·438	0·260	−0·260
IR III	0·112	0·672[a]	0·356	−0·237	−0·104	0·517	−0·071	0·071	−0·741[b]	0·400	0·295	−0·295

AIR: average infiltration rate; SIR: steady infiltration rate; IR I, IR II and IR III: average infiltration rate in stages I, II and III. SOM10, 20 and 30: soil organic matters at the depths of 0–30 cm; SA10, 20 and 30: soil aggregate (>0·25 mm) at the depths of 0–30 cm; BD10, 20 and 30: bulk density at the depths of 0–30 cm; TP10, 20 and 30: soil total porosity at the depths of 0–30 cm; CP10, 20 and 30: soil capillary porosity at the depths of 0–30 cm; NCP10, 20 and 30: soil non-capillary porosity at the depths of 0–30 cm; VWC10, 20 and 30: soil water content at the depths of 0–30 cm; BGB10, 20 and 30: below-ground biomass at the depths of 0–30 cm.
[a]Correlation is significant at the $p < 0{\cdot}05$;
[b]Correlation is significant at the $p < 0{\cdot}01$.

moisture and BD. A total of nine samples were used for laboratory analyses of organic matter content. Moist soil samples were air-dried at room temperature and large roots were removed.

The measurement of SOM content was determined by oxidation with potassium chromate method (Walkley & Black, 1934). Soil BD was measured by a soil bulk sample with a 5-cm diameter and a 5-cm-high stainless steel cutting ring (three replicates). Soil aggregate stability was measured by using a soil aggregate analyser and can measure the percentage of wet sieve aggregates. Using cutting ring method to determine the soil capillary water content (Wc). Soil total porosity (TP), capillary porosity (CP) and non-capillary porosity (NCP) were calculated with the following Equations 1–3 (Jiao *et al*., 2011).

$$TP = \left(1 - \frac{BD}{ds}\right) \times 100 \tag{1}$$

Where: *TP* is the total soil porosity (%); *BD* is the soil bulk density ($\mathrm{g\,cm^{-3}}$); *ds* is the soil particle density ($\mathrm{g\,cm^{-3}}$), in the study *ds* is $2{\cdot}65\ \mathrm{g\,cm^{-3}}$.

$$CP = W_C \times \frac{BD}{V} \times 100 \tag{2}$$

$$NCP = TP - CP \tag{3}$$

Where: *CP* is the soil capillary porosity (%); *Wc* is the soil capillary water content (%); *V* is the volume of soil core ($\mathrm{cm^3}$); *NCP* is the non-capillary porosity (%).

Infiltration Measurement

The automatic soil infiltrability measurement system was applied to determine the complete infiltration processes of different vegetation types (Sun *et al*., 2013; Mao *et al*., 2016; Wu *et al*., 2016b). This method was used for measuring *in situ* infiltration process. We cut the full standing vegetation off at ground level and removed the litter from the soil surface before measuring. This experimental device includes a peristaltic pump, a computer, a camera, a peristaltic pumpsilicone tube and a tripod. The peristaltic pump with a peristaltic pumpsilicone tube was used to supply the constant water flow at a fixed speed to the soil surface, and the design water supply quantity was $2\ \mathrm{L\,h^{-1}}$. The tripod was used to fix the camera. A computer connected with the camera and installed a specific designed software for data measurement. The camera was used to record the advancing processes of wetted soil surface area every 3 min, and the total measurement time was 1.5 h. Mathematical models were used to compute the soil infiltrability from the recorded changes in wetted soil surface area. The infiltration rates at different moments were calculated as follows (Lei *et al*., 2007; Mao *et al*., 2011):

$$\frac{in = q - \sum_{j=1}^{n-1} \mathrm{ij}\ \Delta \mathrm{An} - j + 1}{\Delta An\ (n = 1,\ 2,\ 3, \ldots)} \tag{4}$$

Where: i_n is the soil infiltration rate at time n ($\mathrm{mm\,h^{-1}}$); q is the water flow rate ($\mathrm{L\,h^{-1}}$); ΔA_n is corresponding increased wetted area at the soil surface within time t_n and $t_n - 1$ ($\mathrm{mm^2}$).

According to the dynamic process of infiltration, we divided the process into three different stages (Wu *et al*., 2016). At the start of the 15-min infiltration rate diminished rapidly, what we called the fast infiltration stage, and took the average infiltration rate of 0–15 min as the infiltration rate of this stage (IR I). Afterwards, the decrease of infiltration rate became gently in 15–45 min, what we called the stable change stage, and took the average infiltration rate of 15–45 min as the infiltration rate stage II (IR II). Similarly, in 45–75 min the infiltration rate remained stable and as the third stage of the infiltration process (IR III). We took the last 15 min average infiltration rate as the SIR and 0–90 min average infiltration rate as the average infiltration rate (AIR).

Statistical Analysis

Statistical analysis was conducted by using SPSS 18·0 software (SPSS, 2009). One-way analysis of variance was used to examine the difference significant of soil characteristics and infiltration rate under different grassland types. Significant differences were evaluated at 0·05 level. Correlation analysis was used to study the relativity between infiltration

Table III. (Continued)

	CP20	NCP20	BD30	TP30	CP30	NCP30	VWC10	VWC20	VWC30	BGB10	BGB20	BGB30
AIR	−0·373	−0·135	−0·241	0·241	−0·625[a]	0·423	−0·167	−0·022	−0·165	0·438	0·893[b]	0·912[b]
SIR	−0·237	−0·211	−0·073	0·073	−0·451	0·243	−0·019	0·146	0·035	0·560	0·830[b]	0·825[b]
IR I	−0·497	−0·106	−0·421	0·421	−0·845[b]	0·632[a]	−0·318	−0·245	−0·464	0·259	0·913[b]	0·926[b]
IR II	−0·365	−0·100	−0·239	0·239	−0·581[a]	0·403	−0·171	−0·014	−0·134	0·417	0·855[b]	0·893[b]
IR III	−0·300	−0·147	−0·146	0·146	−0·498	0·309	−0·088	0·077	−0·030	0·497	0·839[b]	0·853[b]

rates and soil characteristics. Stepwise multiple regression was used in determining the primary influence factors of soil characteristics on soil infiltration rate.

RESULTS

Soil Characteristics

The BD and TP had contrary variations among the four grassland types (Table I). The highest TP and NCP were found in *C. korshinskii* shrub-grassland than in other grassland types. The CP was significantly higher in *A. cristatum* and *S. capillata* grasslands than in *M. sativa* and *C. korshinskii* grasslands ($p < 0{\cdot}05$, Table I). SOM content was lowest in *C. korshinskii* shrub-grassland ($18{\cdot}35 \pm 0{\cdot}54$). At soil depth of 0–20 cm, *S. capillata* grassland was improved soil aggregate formation significantly than other three grasslands ($p < 0{\cdot}05$, Table I). The proportion of macroaggregates (>0·25 mm) was highest in *S. capillata* grassland (80·84%), falls by about 18% in *M. sativa* and *A. cristatum* grassland and by 29% in *C. korshinskii* shrub-grassland. At soil depth of 0–10 cm, the highest BGB (1043·9 $g\,m^{-2}$) was found in *M. sativa* grassland, followed by *A. cristatum* (803·2 $g\,m^{-2}$) and *S. capillata* grassland (380·4 $g\,m^{-2}$); the lowest BGB was found in *C. korshinskii* shrub-grassland. While at soil depth of 10–20 cm, the difference between *A. cristatum*, *S. capillata* and *C. korshinskii* was not significant ($p > 0{\cdot}05$, Figure 1) but significantly lower than *M. sativa* ($p < 0{\cdot}05$). At soil depth of 20–30 cm, the BGB in *M. sativa* grassland and *C. korshinskii* shrub-grassland land ($p > 0{\cdot}05$) was approximately four times of that in *A. cristatum* and *S. capillata* grasslands. At depth of 0–30 cm, soil water content increased with the depth of soil layer under the different grassland types (Figure 2). Soil under *A. cristatum* grassland had higher soil water content than those of the *M. sativa*, *S. capillata* grassland and *C. korshinskii* shrub-grassland (Figure 2).

Infiltration Rate under Different Vegetation Types

The infiltration rate decreased significantly at the initial stage and then gradually tends to be stable (Figure 3). The AIR in the *M. sativa* grassland ($37{\cdot}49 \pm 8{\cdot}38\,mm\,h^{-1}$) had no significant difference with *C. korshinskii* shrub-grassland ($31{\cdot}49 \pm 2{\cdot}86\,mm\,h^{-1}$) ($p > 0{\cdot}05$) but was about 30% higher than in the *A. cristatum* ($27{\cdot}31 \pm 4{\cdot}69\,mm\,h^{-1}$) and *S. capillata* ($24{\cdot}31 \pm 1{\cdot}15\,mm\,h^{-1}$) grasslands (Table II). For SIR, the highest value was observed in *M. sativa* grassland ($26{\cdot}87 \pm 6{\cdot}90\,mm\,h^{-1}$), followed by *C. korshinskii* shrub-grassland ($21{\cdot}00 \pm 2{\cdot}42\,mm\,h^{-1}$) and *A. cristatum* grassland ($20{\cdot}27 \pm 4{\cdot}24\,mm\,h^{-1}$); the differences were not significant in the three grasslands ($p > 0{\cdot}05$), while significantly higher than *S. capillata* grassland ($14{\cdot}60 \pm 1{\cdot}11\,mm\,h^{-1}$). Similar changes were also observed for IR I, IR II and IR III. The IR I was higher in *S. capillata* grassland than in the *A. cristatum* grassland.

Correlation between the Infiltration Rate and Soil Characteristics

The infiltration rates were significantly and positively correlated with the SOM at depth of 10–20 cm ($p < 0{\cdot}05$, Table III). Infiltration rates showed weakly and negatively related to the aggregate stability at depth of 0–20 cm. Moreover, at depth of 10–30 cm infiltration rates, were positively correlated with BGB ($p < 0{\cdot}01$). In this study, the BD, TP, NCP and VWC were not significantly correlated with infiltration rates ($p > 0{\cdot}05$), whereas CP was significantly and negatively correlated with the IR I ($p < 0{\cdot}05$). We also concluded that the main factors that affected soil infiltration rates were TP10, CP10, BGB20, BGB30, SOM30 and SA20 (Table IV). The SOM30 and BGB30 were thought to be the positive main influencing factors of AIR and IR III. The values of AIR and IR III were both increased with the increasing of SOM30 and BGB30. Similarly, for SIR and IR II, the BGB20 was the most important factor. The CP10 and NCP10 were negative factors for IR I.

DISCUSSION

Revegetation improved soil characteristics by reducing BD and increasing TP, CP and SOMs (Jiao *et al*., 2011), attributing to the accumulation of fresh plant residues in surface soil as well as decomposed root residues in subsurface soil (Zhao *et al*., 2013). Soil characteristics were closely associated with soil infiltrability (Cerdà, 2001). The combined effects of both structural and topsoil textural porosities increase infiltration and reduce the runoff generation (Alaoui *et al*., 2011). In the present study, we found that the main soil characteristics influenced infiltration rates were BGB, TP, CP, SOMs and soil aggregate. Roots played a most important role in effects soil infiltration, and higher infiltration rate was related to higher BGB. Our results suggested that the infiltration rate was increased with increasing BGB at depth of 10–30 cm. Moreover, the infiltration rates were higher in legume grasslands than gramineous grasslands. We also found that BGB was higher in legume grasslands than gramineous grasslands. Additionally, in shrub-grassland, the majority of the roots concentrated in the upper 10–30 cm of the soil (Costantini *et al*., 2015). These results were in agreement with previous findings regarding the legume grasslands would increase and gramineous grasslands would decrease the infiltration rate (Meek *et al*., 1989; Fischer *et al*., 2014). Previous study has found that in legume grasslands decay of tap roots leave many large channels that increasing infiltration rate (Meek *et al*., 1989; Devitt & Smith, 2002). During the growing season, infiltration rate decreased as tap roots of leguminous fill old root channels, over time infiltration rate increased as roots decay and forming stable macropores, eventually this process would reach an equilibrium point and produce higher infiltration rate (Archer *et al*., 2002; Bodner *et al*., 2008). On the contrary, in gramineous grasslands, fibrous roots tend to grow more densely in clumps within top soil layers and decrease infiltration rate by clogging soil pore space and forming a dense network reducing water movement (Archer *et al*., 2002), which suggested that legume grasslands with tap roots and higher BGB would promote water infiltration compared with gramineous grasslands.

In our study, TP was the vital factor for stable change stage of infiltration rates, and the increased soil porosity would improve infiltration capacity (Fischer *et al*., 2014). Conversely, the CP had a negative effect on infiltration rates of the fast infiltration stage. The CP in gramineous grasslands was greater than in legume grasslands. Indeed, a decrease in infiltration rate is expected if capillary matric fluxes through pores prevail over gravity-driven fluxes. On the other hand, CP has a positive effect on water-holding capacity of soil (Zhao *et al*., 2002).

In our results, SOMs promoted a higher water infiltration in the soil at remained stable stage, and native grasslands had the lowest SOMs and infiltration rates, compared with artificial grasslands. SOMs decreased soil BD and increased soil porosity (Yang *et al*., 2014), thereby conducive to

Table IV. Multiple-regression equations between infiltration rates (AIR, SIR, IRI, IRII and IRIII) and soil characteristics

	Regression equation	R^2
AIR	Y1 = 9·933 + 0·038 BGB30 + 0·679 SOM30	0·992
SIR	Y2 = 14·933 + 0·013 BGB20	0·830
IRI	Y3 = 306·897 − 7·691 CP10 − 1·859NCP10	0·863
IRII	Y4 = -39·319 + 0·018 BGB20 + 1·131 TP10	0·935
IRIII	Y5 = 6·021 + 0·033 BGB30 + 0·793 SOM30 − 0·074 SA20	0·991

AIR: average infiltration rate; SIR: steady infiltration rate; IR I, IR II and IR III: average infiltration rate in stage I, II and III. BGB20 and 30: belowground biomass at the depths of 10–20 and 20–30; SOM30: soil organic matters at the depths of 20–30 cm; TP10: soil total porosity at the depths of 0–10 cm; CP10: soil capillary porosity (>0·25 mm) at the depths of 0–10 cm; NCP10: soil non-capillary porosity at the depths of 0–10 cm; SA20: soil aggregate at the depths of 10–20 cm.
The multiple-regression equations of IRI and soil characteristics were determined at the depth of 0–10 cm; AIR, SIR, IRII and IRIII were determined at the depth of 0–30 cm.

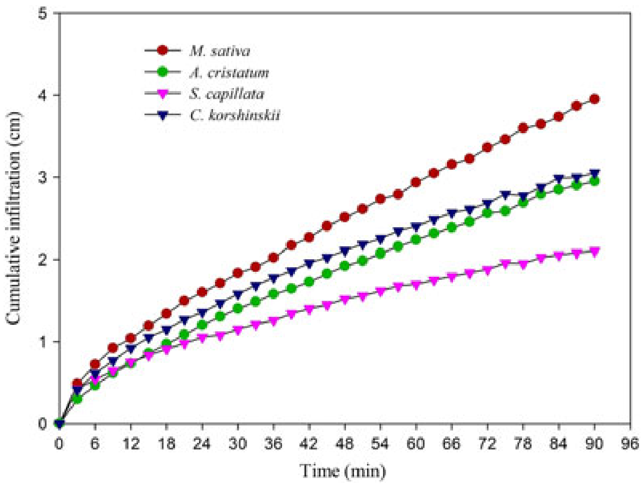

Figure 4. Cumulative infiltration curves for different grasslands. This figure is available in colour online at wileyonlinelibrary.com/journal/ldr

improving the infiltration capacity. Moreover, soil aggregate was higher in native grasslands than artificial grasslands in the top soil, the presence of legumes decreased the soil aggregate (Pérès *et al*., 2013). As a result, the infiltration rate was higher in artificial grasslands than in native grasslands. In contrast to other studies results (Neris *et al*., 2012; Zhao *et al*., 2013), we found that soil aggregate had a negative effect on infiltration rates in remained stable stage. Additionally, the effect of soil aggregate in reducing infiltration rates was largely in gramineous grasslands than legumes grasslands. Some studies suggested that water-stable aggregates render soil water repellency (Rawitz & Hazan, 1978; Giovannini & Lucchesi, 1983; Capriel *et al*., 1995). And water repellency would reduce the infiltration rate (Doerr *et al*., 2000). The cumulative infiltration curve is specific for soil water repellency (Di Prima *et al*., 2016). The soil water repellency was lower in legumes grasslands than gramineous grasslands (Figure 4). Namely, soil aggregate have a negative effect on infiltration rate. Thereby, the higher BGB, SOMs and lower CP and soil aggregate were in favour of water infiltration. The increase in infiltration was of a great importance to promote plant growth and decrease soil erosion in arid environments.

CONCLUSIONS

In the arid regions, legume grasslands showed high infiltration capacity. Higher infiltration capacity of soil was related to increasing BGB, TP, SOMs and lower CP and soil aggregate. Legume grasslands have higher BGB, TP and SOMs than gramineous grasslands; moreover, these factors improved soil infiltration capacity. The results indicated that legume grasslands have greater infiltration rate than gramineous grasslands. In water-restricted regions, it is critical to select the restoration species that are in favour of promoting rainfall infiltration and enhancing soil water storage. Overall, legume grasslands have more adaptability and sustainability in the arid areas.

ACKNOWLEDGEMENTS

We thank Dr Helge Bormann and two anonymous reviewers for his comments and suggestions on this manuscript. This research was funded by the National Natural Science Foundation of China (NSFC41390463, 41525003, and 41371282), the Youth Innovation Promotion Association CAS (2011288), the 'Light of West China' Program of CAS (XAB2015A04), Project of Natural Science Foundation of Shaanxi Province (2014KJXX-15) and Lanzhou Institute of Animal and Veterinary Pharmaceutics Sciences of Chinese Academy of Agricultural Sciences (CAAS-ASTIP-2014-LIHPS-08).

REFERENCES

Abu-Hamdeh NH, Abo-Qudais SA, Othman AM. 2006. Effect of soil aggregate size on infiltration and erosion characteristics. *European Journal of Soil Science* **57**: 609–616. DOI:10.1111/j.1365-2389.2005.00743.x.

Alaoui A. 2015. Modelling susceptibility of grassland soil to macropore flow. *Journal of Hydrology* **525**: 536–546. DOI:10.1016/j.jhydrol.2015.04.016.

Alaoui A, Caduff U, Gerke HH, Weingartner R. 2011. A preferential flow effects on infiltration and runoff in grassland and forest soils. *Vadose Zone Journal* **10**: 367–377. DOI:10.2136/vzj2010.0076.

Angers DA, Caron J. 1998. Plant-induced changes in soil structure: processes and feedbacks. *Biogeochemistry* **42**: 55–72. DOI:10.1023/A:1005944025343.

Archer NAL, Quinton JN, Hess TM. 2002. Below-ground relationships of soil texture, roots and hydraulic conductivity in two-phase mosaic vegetation in south-east Spain. *Journal of Arid Environments* **52**: 535–553. DOI:10.1006/jare.2002.1011.

Bochet E, Poesen J, Rubio JL. 2006. Runoff and soil loss under individual plants of a semi-arid Mediterranean shrubland: influence of plant morphology and rainfall intensity. *Earth Surface Processes and Landforms* **31**: 536–549. DOI:10.1002/esp.1351.

Bodner G, Loiskandl W, Buchan G, Kaul HP. 2008. Natural and management-induced dynamics of hydraulic conductivity along a cover-cropped field slope. *Geoderma* **146**: 317–325. DOI:10.1016/j.geoderma.2008.06.012.

Bormann H, Klaassen K. 2008. Seasonal and land use dependent variability of soil hydraulic and soil hydrological properties of two Northern German soils. *Geoderma* **145**: 295–302. DOI:10.1016/j.geoderma.2008.03.017.

Capriel P, Beck T, Borchert H, Gronholz J, Zachmann G. 1995. Hydrophobicity of the organic matter in arable soils. *Soil Biology and Biochemistry* **27**: 1453–1458. DOI:10.1016/0038-0717(95)00068-P.

Cerdà A. 1996. Seasonal variability of infiltration rates under contrasting slope conditions in southeast Spain. *Geoderma* **69**: 217–232. DOI:10.1016/0016-7061(95)00062-3.

Cerdà A. 1997. Seasonal changes of the infiltration rates in a Mediterranean scrubland on limestone. *Journal of Hydrology* **198**: 209–225. DOI:10.1016/S0022-1694(96)03295-7.

Cerdà A. 2001. Effects of rock fragment cover on soil infiltration, interrill runoff and erosion. *European Journal of Soil Science* **52**: 59–68. DOI:10.1046/j.1365-2389.2001.00354.x.

Costantini EAC, Branquinho C, Nunes A, Schwilch G, Stavi I, Valdecantos A, Zucca C. 2015. Soil indicators to assess the effectiveness of restoration strategies in dryland ecosystems. *Solid Earth Discussions* **7**: 3645–3687. DOI:10.1016/j.geoderma.2008.03.017.

Dabney SM, Delgado JA, Reeves DW. 2001. Using winter cover crops to improve soil and water quality. *Communication Soil Science and Plant Nutrition* **32**: 1221–1250. DOI:10.1081/CSS-100104110.

Daniel DB, Robert AM, Roch EG. 1999. Grassland legume establishment with imazethapyr and imazapic. *Agronomy Journal* **91**: 592–596. DOI:10.2134/agronj1999.914592x.

Devitt DA, Smith SD. 2002. Root channel macropores enhance downward movement of water in a Mojave Desert ecosystem. *Journal of Arid Environments* **50**: 99–108. DOI:10.1006/jare.2001.0853.

Di Prima S, Lassabatère L, Bagarello V, Iovino M, Angulo-Jaramillo R. 2016. Testing a new automated single ring infiltrometer for Beerkan infiltration experiments. *Geoderma* **262**: 20–34. DOI:10.1016/j.geoderma.2015.08.006.

Doerr SH, Shakesby RA, Walsh RPD. 2000. Soil water repellency: its causes, characteristics and hydro-geomorphological significance. *Earth-Science Reviews* **51**: 33–65. DOI:10.1016/S0012-8252(00)00011-8.

Fischer C, Roscher C, Jensen B, Eisenhauer N, Baade J, Attinger S, Scheu S, Weisser WW, Schumacher J, Hildebrandt A. 2014. How do earthworms, soil texture and plant composition affect infiltration along an experimental plant diversity gradient in grassland? *Plos One* **9**: e98987–e98987. DOI:10.1371/journal.pone.0098987.

Franzluebbers AJ. 2002. Water infiltration and soil structure related to organic matter and its stratification with depth. *Soil and Tillage Research* **66**: 197–205. DOI:10.1016/S0167-1987(02)00027-2.

Giovannini G, Lucchesi S. 1983. Effect of fire on hydrophobic and cementing substances of soil aggregates. *Soil Science* **136**: 231–236. DOI:10.1097/00010694-198310000-00006.

Gonzalez-Sosa E, Braud I, Dehotin J, Lassabatère L, Angulo-Jaramillo R, Lagouy M, Branger F, Jacqueminet C, Kermadi S, Michel K. 2010. Impact of land use on the hydraulic properties of the topsoil in a small French catchment. *Hydrological Processes* **24**: 2382–2399. DOI:10.1002/hyp.7640.

Hu W, Shao MA, Wang QJ, Fan J, Horton R. 2009. Temporal changes of soil hydraulic properties under different land uses. *Geoderma* **149**: 355–366. DOI:10.1016/j.geoderma.2008.12.016.

Jiao F, Wen ZM, An SS. 2011. Changes in soil properties across a chronosequence of vegetation restoration on the Loess Plateau of China. *Catena* **86**: 110–116. DOI:10.1016/j.catena.2011.03.001.

Kodešová R, Jirků V, Kodeš V, Mühlhanselová M, Nikodem A, Žigová A. 2011. Soil structure and soil hydraulic properties of Haplic Luvisol used as arable land and grassland. *Soil and Tillage Research* **111**: 154–161. DOI:10.1016/j.still.2010.09.007.

Lal R. 1996. Deforestation and land-use effects on soil degradation and rehabilitation in western Nigeria. I. Soil physical and hydrological properties. *Land Degradation & Development* **7**: 19–45. DOI:10.1002/(SICI)1099-145X(199603)7: 1<19::AID-LDR212> 3.0.CO;2-M.

Lei TW, Mao LL, Li X, Liu H, Huang XF, Zhang YN. 2007. Method for measuring soil infiltrability with linear run-on of water. *Transactions of the Chinese Society of Agricultural Engineering* **23**: 1–5. DOI:10.3969/j.issn.1002-6819.2007.1.001.

Leung AK, Garg A, Coo JL, Ng CWW, Hau BCH. 2015. Effects of the roots of *Cynodon dactylon* and *Schefflera heptaphylla* on water infiltration rate and soil hydraulic conductivity. *Hydrological Processess* **29**: 3342–3354. DOI:10.1002/hyp.10452.

Liu CM, Chen YN, Xu ZX. 2010. Eco-hydrology and sustainable development in the arid regions of China preface. *Hydrological Processes* **24**: 127–128. DOI:10.1002/hyp.7481.

Mao D, Cherkauer KA. 2009. Impacts of land-use change on hydrologic responses in the Great Lakes region. *Journal of Hydrology* **374**: 71–82. DOI:10.1016/j.jhydrol.2009.06.016.

Mao LL, Lei TW, Bralts VF. 2011. An analytical approximation method for the linear source soil infiltrability measurement and its application. *Journal of Hydrology* **411**: 169–177. DOI:10.1016/j.jhydrol.2011.08.066.

Mao LL, Li YZ, Hao WP, Mei XR, Bralts VF, Li HR, Gao R, Lei TW. 2016. An approximate point source method for soil infiltration process measurement. *Geoderma* **264**: 10–16. DOI:10.1016/j.geoderma.2015.09.011.

Mchunu CN, Chaplot V. 2012. Land degradation impact on soil carbon losses through water erosion and CO_2 emissions. *Geoderma* **177–178**: 72–79. DOI:10.1016/j.geoderma.2012.01.038.

McIvor JG, Williams J, Gardener CJ. 1995. Pasture management influences runoff and soil movement in the semi-arid tropics. *Australian Journal of Experimental Agriculture* **35**: 55–65. DOI:10.1071/EA9950055.

Meek BD, Rechel EA, Carter LM, DeTar WR. 1989. Changes in infiltration under alfalfa as influenced by time and wheel traffic. *Soil Science Society of America Journal* **53**: 238–241. DOI:10.2136/sssaj1989.03615995005300010042x.

Neris J, Jiménez C, Fuentes J, Morillas G, Tejedor M. 2012. Vegetation and land-use effects on soil properties and water infiltration of Andisols in Tenerife (Canary Islands, Spain). *Catena* **98**: 55–62. DOI:10.1016/j.catena.2012.06.006.

Pérès G, Cluzeau D, Menasseri S, Soussana JF, Bessler H, Engels C, Scheu S. 2013. Mechanisms linking plant community properties to soil aggregate stability in an experimental grassland plant diversity gradient. *Plant and Soil* **373**: 285–299. DOI:10.1007/s11104-013-1791-0.

Podwojewski P, Janeau JL, Grellier S, Valentin C, Lorentz S, Chaplot V. 2011. Influence of grass soil cover on water runoff and soil detachment under rainfall simulation in a sub-humid South African degraded rangeland. *Earth Surface Processes and Landforms* **36**: 911–922. DOI:10.1002/esp.2121.

Rawitz E, Hazan A. 1978. The effect of stabilized, hydrophobic aggregate layer properties on soil water regime and seedling emergence. *Soil Science Society of America Journal* **42**: 787–793. DOI:10.2136/sssaj1978.03615995004200050028x.

Rodriguez-Iturbe I. 2000. Eco-hydrology: a hydrologic perspective of climate-soil-vegetation dynamics. *Water Resources Research* **36**: 3–9. DOI:10.1029/1999WR900210.

Siltecho S, Hammecker C, Sriboonlue V, Clermont-Dauphin C, Trelo-Ges V, Antonino ACD, Angulo-Jaramillo R. 2015. Use of field and laboratory methods for estimating unsaturated hydraulic properties under different land uses. *Hydrology and Earth System Sciences* **19**: 1193–1207. DOI:10.5194/hess-19-1193-2015.

SPSS. 2009. PASW statistics for windows, version 18.0. SPSS Inc.: Chicago.

Sun B, Mao LL, Zhao J, Lei TW. 2013. Effects of flow rate on soil infiltrability measurement with the automatic system. *Science of Soil Water Conservation* **11**: 14–18. DOI:10.3969/j.issn.1672-3007.2013.02.003.

Vervoort RW, Dabney SM, Römkens MJM. 2001. Tillage and row position effects on water and solute infiltration characteristics. *Soil Science Society of America Journal* **65**: 1227–1234. DOI:10.2136/sssaj2001.6541227x.

Wahl NA, Bens O, Schäfer B, Hüttl RF. 2003. Impact of changes in land-use management on soil hydraulic properties: hydraulic conductivity, water repellency and water retention. *Physics and Chemistry of the Earth, Parts A/B/C* **28**: 1377–1387. DOI:10.1016/j.pce.2003.09.012.

Walkley A, Black IA. 1934. An examination of the Degtjareff method for determining soil organic matter, and a proposed modification of the chromic acid titration method. *Soil Science* **37**: 29–38. DOI:10.1097/00010694-193401000-00003.

Wang XP, Li XR, Xiao HL, Berndtsson R, Pan YX. 2007. Effects of surface characteristics on infiltration patterns in an arid shrub desert. *Hydrological Processes* **21**: 72–79. DOI:10.1002/hyp.6185.

Wang Y, Fan J, Cao L, Liang Y. 2016. Infiltration and runoff generation under various cropping patterns in the red soil region of China. *Land Degradation & Development* **27**: 83–91. DOI:10.1002/ldr.2460.

Weiler M, Naef F. 2003. An experimental tracer study of the role of macropores in infiltration in grassland soils. *Hydrological Processes* **17**: 477–493. DOI:10.1002/hyp.1136.

Wu GL, Liu Y, Tian FP, Shi ZH. 2016a. Legumes functional group promotes soil organic carbon and nitrogen storage by increasing plant diversity. *Land Degradation & Development* . DOI:10.1002/ldr.2570.

Wu GL, Yang Z, Cui Z, Liu Y, Fang NF, Shi ZH. 2016b. Mixed artificial grasslands with more roots improved mine soil infiltration capacity. *Journal of Hydrology* **535**: 54–60. DOI:10.1016/j.jhydrol.2016.01.059.

Yang F, Zhang GL, Yang JL, Li DC, Zhao YG, Liu F, Yang RM, Yang F. 2014. Organic matter controls of soil water retention in an alpine grassland and its significance for hydrological processes. *Journal of Hydrology* **519**: 3086–3093. DOI:10.1016/j.jhydrol.2014.10.054.

Yu MZ, Zhang LL, Xu XX, Feger KH, Wang YH, Liu WZ, Schwarzel K. 2015. Impact of land-use changes on soil hydraulic properties of Calcaric Regosols on the Loess Plateau, NW China. *Journal of Plant Nutrition and Soil Science* **178**: 486–498. DOI:10.1002/jpln.201400090.

Zhao SW, Zhou YD, Wu JS. 2002. Soil moisture characteristics of different vegetations in northern of Ziwuling. *Journal of Soil Water Conservation* **16**: 119–122. DOI:10.3321/j.issn:1009-2242.2002.04.031.

Zhao YG, Wu PT, Zhao SW, Feng H. 2013. Variation of soil infiltrability across a 79-year chronosequence of naturally restored grassland on the Loess Plateau, China. *Journal of Hydrology* **504**: 94–103. DOI:10.1016/j.jhydrol.2013.09.039.